Proceedings of the ASME 2010 3rd Joint US-European Fluids Engineering Summer Meeting and 8th International Conference on Nanochannels, Microchannels, and Minichannels
FEDSM-ICNMM2010
August 1-5, 2010, Montreal, Canada

FEDSM-ICNMM2010-31252

PNEUMATICALLY ACTUATED DIAPHRAGM SINGLE CHAMBER MICROPUMP

Son H. Ho[a,b], Muhammad M. Rahman[b], Srinivas Katkoori[c], Ashit Talukder[d,e]
[a]Department of Mechanical, Materials and Aerospace Engineering, University of Central Florida, Orlando, Florida, USA
[b]Department of Mechanical Engineering, University of South Florida, Tampa, Florida, USA
[c]Department of Computer Science and Engineering, University of South Florida, Tampa, Florida, USA
[d]NASA Jet Propulsion Laboratory, California Institute of Technology, Pasadena, California, USA
[e]University of Southern California, Los Angeles, California, USA

ABSTRACT

The analysis of a single chamber micropump with a diaphragm driven by a pulse train of external pressure and two passive check valves at inlet and outlet is performed. The model for the micropump is developed based on the fundamentals of fluid mechanics and theory of plates with quasi-static approximation. The simulation results are compared with existing experimental data. They are in good agreement on flow rate and in reasonable agreement on backpressure for low driving frequency up to 3 Hz. It is found that the flow rate increases as the driving frequency increases or the backpressure decreases. The results also predict that a duty cycle of 50% results in the highest flow rate at the same frequency and actuating pressure. Also, a higher actuating pressure yields a higher flow rate. The model presented here can effectively assist the design process of micropumps since the model is directly related to the basic design parameters such as geometric dimensions and material properties.

INTRODUCTION

Microfluidic systems are used for a variety of applications in biology, medicine, microelectronics cooling, and space exploration. Micropumps are used in many of these systems. Micropumps have been developed and studied for almost three decades following various goals and approaches [1]. Shoji and Esashi [2] presented a review on microflow devices from the point of view of actuating principles and structures with micropumps included as a part besides microvalves and microflow sensors. As the microfluidics field expanded over time, micropump became a growing research field with a significant number of literatures published. A review paper dedicated only to MEMS-micropumps was prepared by Nguyen et al. [3]. Micropump principles and their realization with MEMS-technology were introduced. Pump size, flow rate, and backpressure of existing micropumps were compared. The most up-to-date and thorough review on micropumps was presented by Laser and Santiago [1]. It provides a reference on principles and comparison of design and operation parameters of a large number of micropumps. The pumps can be classified into two main categories as displacement and dynamic micropumps. Reciprocating displacement micropumps have been extensively studied, fabricated with many types of actuators and valve configurations. They are usually equipped with a deformable plate with fixed edges as the pump diaphragm that serves as a reciprocating moving surface which exerts periodic work done on the working fluid and produces the pumping effect, and therefore also called diaphragm micropumps [1].

Figure 1(a) shows a schematic of a system with a micropump that pumps the working fluid from the source reservoir to the destination reservoir. The micropump has a main chamber bounded by a diaphragm on one side and by an inlet and an outlet passive check valves on the other. The two check valves allow the fluid to flow only one way, in or out of the main chamber. The diaphragm is an elastic plate with fixed edges that deflects up and down under an actuating load applied by an actuation mechanism. During operation, the actuating load acts periodically on the diaphragm and forces it to deflect and thus alternately increase and decrease the volume of the chamber. As the volume of the pump chamber decreases as shown in Fig. 1(b), chamber pressure increases until it opens the outlet valve and the working fluid is forced out of the pump chamber in a stroke designated as "compression/discharge stroke." The difference between the compression stage and the discharge stage of this stroke is that the outlet valve is still closed during the former and open during the latter. The volume of the chamber at the lowest position of the diaphragm is called the dead volume. Similarly, as the chamber volume increases as shown in Fig. 1(c), the working fluid is drawn into the pump chamber in a stroke designated as "expansion/suction stroke." As the diaphragm moves from the lowest to the highest position, it sweeps a volume called the stroke volume.

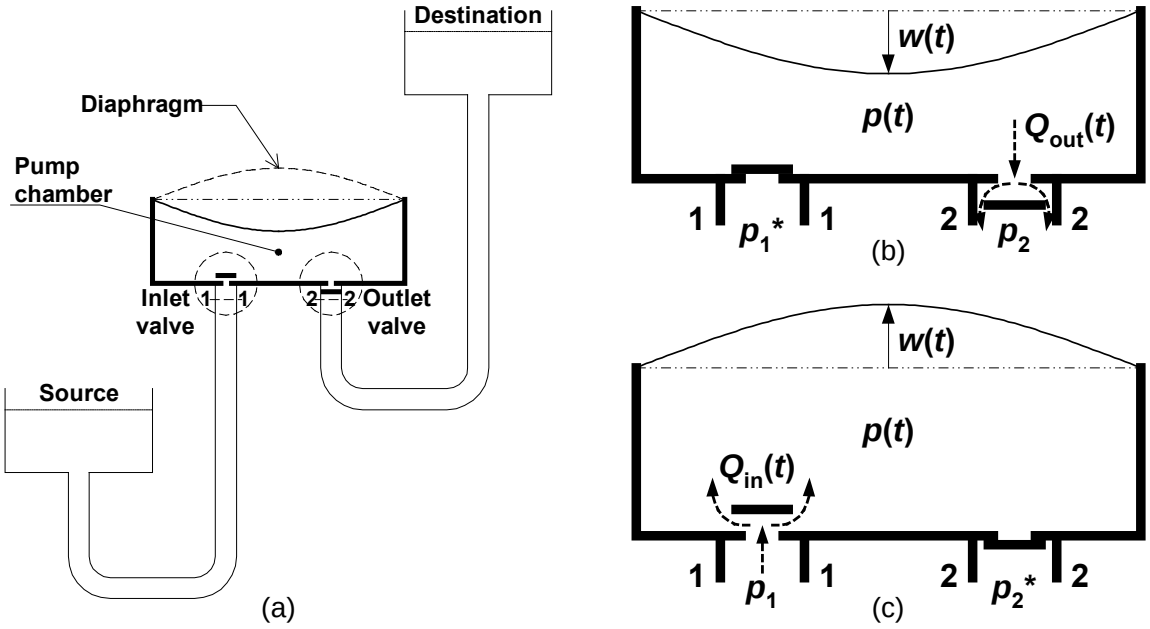

Figure 1 Operation of a typical diaphragm micropump with passive check valves: (a) Complete fluid pumping system; (b) Compression/discharge stroke; (c) Expansion/suction stroke.

It can be noted that there are also multiple chamber configurations where the micropump has two or three pump chambers in series. Each diaphragm operates in particular sequence that is out-of-phase with the others to produce the pumping effect. Thus, they are also referred to as peristaltic micropumps [4-6] or micropumps with active valves [7,8]. However, the operating principle of this type of micropumps is quite different from those with single chamber and passive check valves where the valves are opened and closed by the chamber pressure, not by actuation mechanisms. This study considers a micropump that has a single chamber with a reciprocating diaphragm and two passive check valves at inlet and outlet, referred to as "micropump" in this paper for convenience.

Although there are recently hundreds of research articles on the subject, only a few of them are fully or partly dedicated to modeling and simulation of the operation of micropump, and the use of that in design. Richter et al. [9] presented a simple approach on robust design of micropumps for liquid and gas based on only a few parameters such as dead volume, stroke volume, critical pressure of valves, and compressibility of the working fluid. They developed design rules to give a general guideline for compression ratio required. However, no simulation can be gained from this approach. Zengerle and Richter [10] studied the dynamic behavior of microfluidic devices including diaphragm micropumps, microvalves, and microchannels, and developed basic and extended models for micropump operation. Morris and Forster [11] presented low-order modeling for fixed-valve micropumps using electrical network equivalent. Bourouina and Grandchamp [12] used electrical equivalent networks to model membrane micropumps with double check valves. Olsson et al. [13] presented a numerical design study based on lump-mass model (control volume) for a valveless diffuser micropump. Moussa and Gonzalez [14] used Finite Element Analysis (FEA) with the software ALGOR (ALGOR, Inc., currently, Autodesk, Inc.) to simulate the dynamic response of a piezoelectric-driven membrane. Morris and Forster [15] also employed FEA with the software ANSYS (ANSYS, Inc.) for the optimization of a circular piezoelectric bimorph. Gerlach [16] studied micro diffuser channel as dynamic passive valves for micropumps using hydrodynamics with empiro-theoretical approach. Ullman and Fono [17] developed an improved dynamic model for a piezoelectric valveless pump. Pan et al. [18] considered inertial effects in valveless micropump by studying the differential equations governing the fluid flow and fluid-membrane coupling through flow field simplification. Gamboa et al. [19] studied and optimized fixed-geometry valves of Tesla element type for micropumps. Koch et al. [20] presented a new design for a silicon-based micropump with a quasi-static simulation using ANSYS coupled with FLOW3D. The piezoelectric membrane deflection was simulated with ANSYS. A differential equation for the combined actuation of membrane and valves was solved numerically with Maple (Maplesoft, Waterloo Maple, Inc.).

In general, it can be observed that the FEA approach is employed for simulating the response of the diaphragm under actuating force in most cases. The mathematical models for micropumps of various configurations found from relevant literatures range from simplified electrical network analogies to sophisticated high-order partial differential equation. It can be difficult for one who is looking for guidelines to design a

micropump and verify its performance from such diversified and not very design-oriented information. It is necessary to develop a consistent approach to the modeling and simulation that can assist the design of micropumps.

The objective of this paper is to present a modeling approach that explicitly and directly relates the basic design parameters to the performance of the micropump. The resulting model can be used for simulating the operation of the micropump as well as for verifying if the chosen values for the design parameters result in expected performance of the micropump. For the simplicity of a first order approximation, a quasi-static operation of the micropump is considered. This assumption certainly limits the applicable range of the model to low frequency, which is still useful in certain fields such as drug delivery. On the other hand, the intended flexibility of the model allows future extensions to more accurate models without too much effort. First, a mathematical model for a diaphragm micropump actuated by pneumatic pressure from an external source is formulated. Then, it is implemented on Simulink (The MathWorks, Inc.), a computer simulation graphical-interactive environment for system described by ordinary differential equations. The model is validated with experimental data from Meng et al. [21]. Simulation results are presented. Parametric studies are also performed and reported.

MATHEMATICAL MODEL

Geometric characteristics of pump chamber

The volume of a pump chamber changes during operation as the diaphragm deflects. The nominal volume V_0 is defined as the volume when the diaphragm is flat or has zero deflection. A micropump chamber is usually composed of many connected compartments formed by inside sub-structures such as valve seats whose sizes are significant compared to the volume of the major part of the chamber itself. Nominal volume of a pump chamber can be calculated from a detail drawing of the chamber if one exists. However, during preliminary design phase, such information has not yet been available and V_0 itself is a parameter being designed. In order to relate V_0 to the other design parameters, a base area is chosen as the area A of the diaphragm at zero deflection. This base area will emerge later in the formula for the displacement volume created by the deflection of the diaphragm. The nominal volume of a pump chamber can be characterized by an equivalent height h defined as

$$h = \frac{V_0}{A} \tag{1}$$

Under the effects of the actuating load (for example, pressure), the diaphragm deflects and forms a deflection surface. The shape of the deflection surface is dictated by the diaphragm edge fixity and the loading configuration. The displacement volume created by a deflected diaphragm sweeping from its flat position (zero deflection) can be expressed as

$$V_{\mathrm{d}} = \zeta A w \tag{2}$$

In Eq. (2), w is the deflection at the center of the diaphragm and ζ is named the diaphragm deflection-volume factor. The factor ζ is dependent on the configuration of the actuation mechanism that includes the edge fixity of the diaphragm and actuating load type. For shapes of simple geometry such as cylinder or cone, ζ can be directly deduced from volume formulae. Otherwise, it can be found from the solutions of deflection surfaces of diaphragms with respect to different cases of loading and boundary conditions. Analytical solutions for most of the deflection surfaces of circular and rectangular diaphragms subjected to load uniformly distributed or concentrated at center with clamped or simply supported edges can be found from textbooks in theory of plates and shells such as Ugural [22] or Timoshenko and Woinowsky-Krieger [23]. Numerical solution methods are also presented in these textbooks and can be employed for cases where analytical solution is not available. For convenience, from now on, the term “deflection” refers to “deflection at the center of the diaphragm” w, unless stated otherwise. The positive direction of the deflection w is designated as the one that decreases the volume of the pump chamber.

Figure 2 shows several examples of volume factor ζ for various cases of volumes of circular base. The cylinder shown in Fig. 2(a) represents the displacement volume created by a piston of area A as it moves one stroke of w in its cylinder. It can be taken as the reference case with $\zeta = 1$. With the same A and w, because of its fixed edges, the displacement volume created by a diaphragm is always smaller than that by a piston, that is, $\zeta < 1$. The factor ζ can be understood as the ratio of the volume of a particular deflection surface to that of the reference cylinder. Figure 2(b) shows a cone that approximates the shape of a highly flexible diaphragm subjected to a force concentrated at center. Figure 2(c) and (d) are for circular diaphragms subjected to uniform load (for example, pressure) with clamped edge and simply supported edge, respectively. The clamped edge case in Fig. 2(c) has $\zeta = 1/3$ or 0.33, whereas the simply supported edge case in Fig. 2(d) has a higher value of ζ, dependent on the Poisson's ratio ν of the diaphragm material but not exceeding 7/15 or 0.47. These two cases are the two extreme types of boundary condition for a diaphragm: most and least restrained, respectively. Since realistic support members or fixing mechanisms tolerate some degree of flexibility, no exact edge condition is likely to be realized, and a condition of true edge fixity is especially difficult to obtain [24]. In a practical point of view, ζ can be expressed as an increasing function of w as the latter varies from small deflection zone to large deflection zone. Since ζ varies within a small range of about 0.33–0.47, it can be considered as a constant in most cases and a median value of $\zeta = 0.4$ can be used as a compromise for a partially restrained edge condition.

From Eqs. (1) and (2), the instantaneous volume V of a micropump chamber can be expressed as

$$V = V_0 - V_{\mathrm{d}} = Ah - \zeta A w = A(h - \zeta w) \tag{3}$$

In Eq. (3), the geometric parameters A and h are constants for a particular design, and ζ in general is a function of w that can be considered as a constant of 0.4 for this study. Equation (3) represents the volume of the micropump chamber V as a function of the deflection w of the diaphragm, which, in turn, is a function of time t controlled by an actuating mechanism. Therefore, deflection as a single function of time $w(t)$ that describes the reciprocating motion of a diaphragm is sufficient to model the periodic change in volume of the pump chamber that produces the pumping effect.

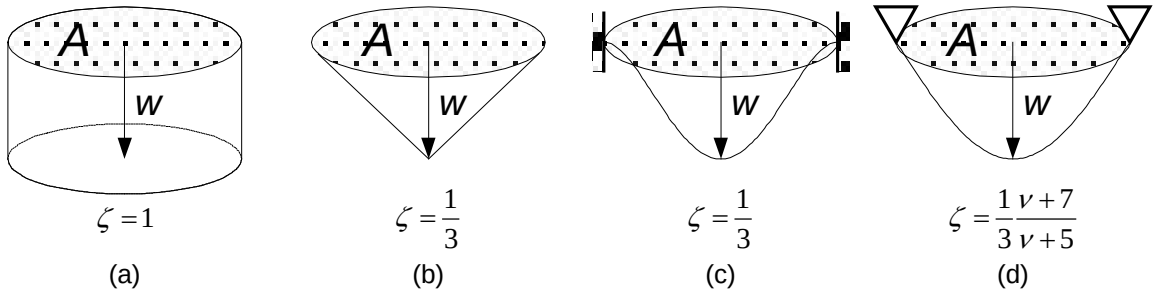

$\zeta = 1$ (a) $\quad \zeta = \frac{1}{3}$ (b) $\quad \zeta = \frac{1}{3}$ (c) $\quad \zeta = \frac{1}{3}\frac{\nu+7}{\nu+5}$ (d)

Figure 2 Diaphragm factors for volumes of deflection surface with circular base: (a) cylinder; (b) cone; circular plate under uniform load with (c) clamped edge, and (d) simply supported edge.

Equation for pressure in pump chamber

The conservation of mass applied to the liquid body inside the pump chamber as a control volume with moving boundary, followed by some mathematical manipulations, yields

$$\rho\left(\frac{V}{K}\frac{\mathrm{d}p}{\mathrm{d}t}+\frac{\mathrm{d}V}{\mathrm{d}t}\right)=\rho_{\text{in}}Q_{\text{in}}-\rho_{\text{out}}Q_{\text{out}} \tag{4}$$

The bulk modulus K of a fluid is a thermodynamic property that represents the change of density with increasing pressure [25]. For liquids, K can be considered as constant since it only varies slightly with pressure and temperature.

In the right hand side of Eq. (4), the instantaneous flow rates through the inlet and outlet are functions of the pressure differences at the respective check valves, and can be represented as

$$Q_{\text{in}}=\Phi_1(p_1-p) \tag{5}$$

$$Q_{\text{out}}=\Phi_2(p-p_2) \tag{6}$$

Φ_1 and Φ_2 are characteristic functions (flow rate versus pressure difference) of the check valves and can be determined in separate studies for the valves alone. In this paper, these functions are obtained from a regression analysis on the experimental data reported by Meng et al. [21].

Assuming that density of the inflow and the outflow is approximately the same as that of fluid in the pump chamber, substituting Eqs. (3), (5) and (6) into Eq. (4), followed by some mathematical manipulations, yields

$$\frac{\mathrm{d}p}{\mathrm{d}t}=\frac{K}{A(h-\zeta w)}\left[\Phi_1(p_1-p)-\Phi_2(p-p_2)+A\zeta\frac{\mathrm{d}w}{\mathrm{d}t}\right] \tag{7}$$

Large deflection of diaphragm under pressure

In micropump operation, the diaphragm usually endures deflections of several times larger than its thickness. Therefore, large deflection theory should be used. Employing approximate method for circular plate in large deflection with pre-stressed tension included [22], pressure difference can be expressed as a function of deflection as

$$p=p_a-B_1w-B_2w^3 \tag{8}$$

where

$$B_1=\frac{16}{3}\frac{E}{1-\nu^2}\frac{\delta^3}{a^4}+\frac{4\sigma_0\delta}{a^2} \tag{9}$$

$$B_2=\frac{8}{3}\frac{E}{1-\nu}\frac{\delta}{a^4} \tag{10}$$

Governing equation for pneumatically actuated diaphragm micropump

Substituting Eq. (8) into Eq. (7), followed by some mathematical manipulations, yields

$$\frac{\mathrm{d}w}{\mathrm{d}t}=\frac{K\left[\Phi_1(p_1-p)-\Phi_2(p-p_2)\right]}{A\left(C_0+C_1w+C_2w^2+C_3w^3\right)} \tag{11}$$

where

$$C_0=-\zeta K-hB_1 \tag{12}$$

$$C_1=\zeta B_1 \tag{13}$$

$$C_2 = -3hB_2 \tag{14}$$

$$C_3 = 3\zeta B_2 \tag{15}$$

Equation (11) is a nonlinear first-order ordinary differential equation of w as a function of t. Once the solution of w is found, pressure in pump chamber can be found from Eq. (8); and inlet and outlet instantaneous flow rates can be found from Eqs. (5) and (6), respectively. The cumulative fluid volume pumped in and out of the pump chamber during one pump cycle τ can be expressed as

$$G_1 = \int_0^\tau \Phi_1 \, \mathrm{d}t \tag{16}$$

$$G_2 = \int_0^\tau \Phi_2 \, \mathrm{d}t \tag{17}$$

For a stationary pumping operation, the cumulative inflow and outflow fluid volumes should be the same, that is $G_1 = G_2 = G$. The flow rate of the micropump can be expressed as

$$Q = fG \tag{18}$$

NUMERICAL SOLUTION

For the validation of the model, the relevant numerical values of the parameters in Eq. (11) are taken from the experimental study on the operation of a check-valved silicone diaphragm micropump developed by Meng et al. [21]. The parameters that are not explicitly reported are estimated by making inferences from available known information. Data on geometric dimensions of the pump structure and physical properties of the materials (diaphragm of silicone rubber, water as working fluid) are adopted or estimated as follows: a = 4 mm, h = 2 mm, δ = 0.14 mm, E = 0.51 MPa, ν = 0.5, K = 2.23 GPa, ζ = 0.4. For the value of K of the working fluid (water), it is assumed that the micropump is well primed, that is, the working fluid within the chamber is liquid water without air bubbles.

The characteristic functions of the check valves can be obtained from the experimental data from Meng et al. [21] as shown in Fig. 3. The flow rate through the inlet or outlet check valve as a function of pressure difference are found using linear regression as

$$\begin{aligned}\Phi(\Delta p) &= \begin{cases} 0.033(\Delta p - 715) & \Delta p > 715 \\ 0 & \Delta p \le 715 \end{cases} \\ &= 0.033(\Delta p - 715)\mathrm{H}(\Delta p - 715)\end{aligned} \tag{19}$$

where H is the unit step function (also known as the Heaviside function).

From Eq. (19), the forward flow amplification factor and the critical pressure of the inlet and outlet check valves are found as $D_1 = D_2$ = 0.033 μL/Pa, $p_{v1} = p_{v2} = p_v$ = 715 Pa.

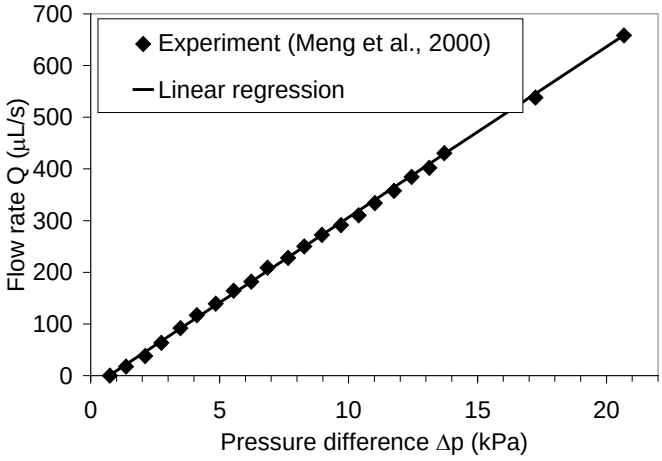

Figure 3 Characteristic curve of check valve (experimental data from [4]).

A base case is set with the following base values of the operating parameters: $p_1 = p_2 = 0$, p_v = 715 Pa, p_a = 6900 Pa, f = 1 Hz (or τ = 1 s), ϕ = 50%. The simulations for parametric studies are based on the base case with some parameters vary from their base values. It is assumed that the diaphragm is initially at zero deflection, $w = 0$, while pressure on both of its sides also is zero, $p = p_a = 0$, and both check valves are closed.

There are various methods for solving an ordinary differential equation as Eq. (11). Although Eq. (11) appears to be variable separable, which is potential for an analytical solution, it is unlikely that such analytical solution exists since the forms of the check valve characteristic functions can be complicated with rectifying effect and possible reverse leaking. In order to develop a robust model that can be able to extend to similar micropump configurations, numerical solution is a better choice to solve Eq. (11). For solving a nonlinear first-order ordinary differential equation, many numerical methods such as the well-known Runge-Kutta method and its alternatives have been developed for over a century. Although an in-house code implementing one of these numerical methods can be programmed on any programming languages (C, FORTRAN, etc.) to solve Eq. (11), it is convenient to use Simulink (The MathWorks, Inc.) to build the numerical model with the block diagram that explicitly and clearly represents the relationships between the design parameters and variables.

Figure 4 presents the Simulink model that implements the mathematical model of the micropump, Eqs (8) through (15), including the characteristic functions of the check-valves, Eq. (19). Most of the design parameters such as geometric dimensions, material properties, and operation parameters are arranged in one column to the left of the block diagram. This allows the parameters to be conveniently assigned different values during analysis or design processes. Implementations of

Eqs. (16) and (17) for fluid volume pumped in and out in one pump cycle are also included.

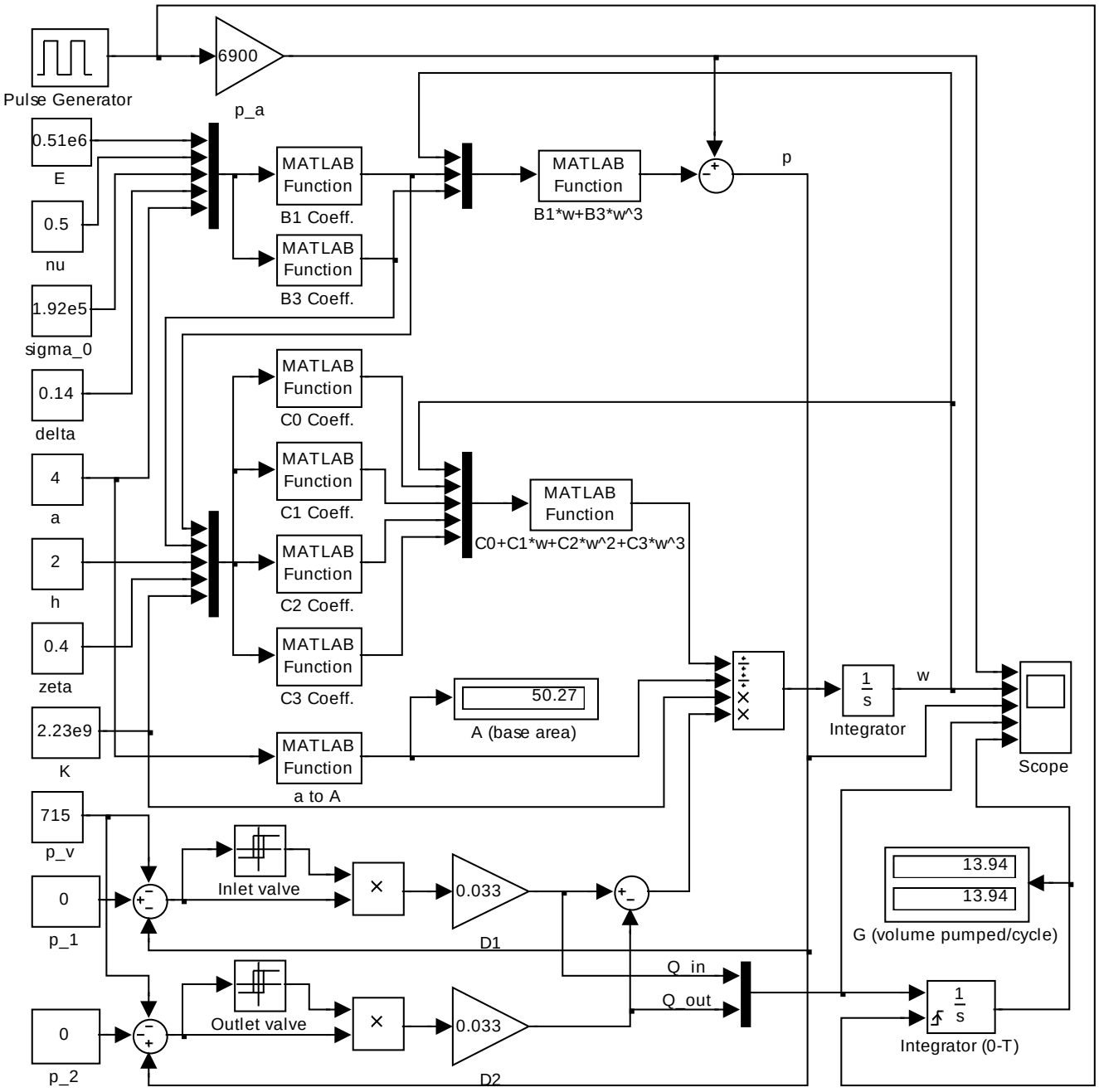

Figure 4 Simulink model (The MathWorks, Inc.) of pneumatically actuated micropump.

RESULTS AND DISCUSSION

Figure 5 shows the simulation results for the base case: actuating pressure of p_a = 6.9 kPa at pump frequency of f =1 Hz and duty cycle of ϕ = 50% and zero backpressure p_2 = 0. In Fig. 5(a), (b), and (c), the actuating pressure p_a, the diaphragm deflection w, and the pump chamber pressure p are presented as functions of time. They are to be analyzed simultaneously to study the operation of the pump. As the actuating pressure increases immediately from zero to peak value (6.9 kPa) in only a moment corresponding to the rising edge of the control pulse, the diaphragm has no time to move and thus remains at its position while pump chamber pressure p increases reactively to peak value. This is the compression stage of the pump operation where p increases without any fluid flow. As the pressure difference at outlet is higher than its critical pressure, $p - p_2 > p_{v2}$, the outlet valve is opened and fluid flows through it out of the chamber. This outflow causes chamber pressure to decrease as actuating pressure holds its peak value; while diaphragm

deflection increases (which reduces the volume of pump chamber). This is the discharge stage where the fluid is driven out by pressure difference and a volume is displaced by the deflecting diaphragm until $p - p_2 = p_{v2}$ when the outflow stops at the end of the duty cycle of actuating pressure. In the second half of an actuating cycle, actuating pressure is removed. It decreases from peak value to zero along the falling edge of the control pulse in a very short time. Without external pressure, the diaphragm tends to return to its flat position due to its material elasticity. As the diaphragm retracts, it creates vacuum in the pump chamber. This constitutes the expansion stage. As the pressure difference at inlet is higher than its critical pressure, $p_1 - p > p_{v1}$, the inlet valve is opened and allows fluid to flow into the chamber. This inflow causes chamber pressure to increase as the diaphragm retracts further toward its zero deflection position while actuating pressure remains at zero. This is the suction stage where the fluid is sucked in by pressure difference and a volume is displaced by the deflecting diaphragm until $p_1 - p = p_{v1}$ when the inflow stops at the end of the cycle of actuating pressure. The rising edge of the next actuating pressure pulse starts next pump cycle.

Figure 5(d) shows the resulting instantaneous flow rate of the inflow and outflow. As expected, they are in anti-phase with each other due to the nature of the operation where suction and discharge occur in different strokes of the diaphragm resulting that the inflow and outflow never overlap, assuming that backward leaking at the check valves can be neglected. Their graphs has the same shape due to the symmetry of the actuating pressure pulse of 50% duty cycle. They both increase from zero to their peak values in a very short time at the starts of their actuating stages, and then sharply decrease along curving paths to zero at the end of these stages. The higher peak of outlet flow rate in the first cycle represents the transient response as the diaphragm performs the first down stroke and drives out excess fluid volume before the pump reaches its stationary operation.

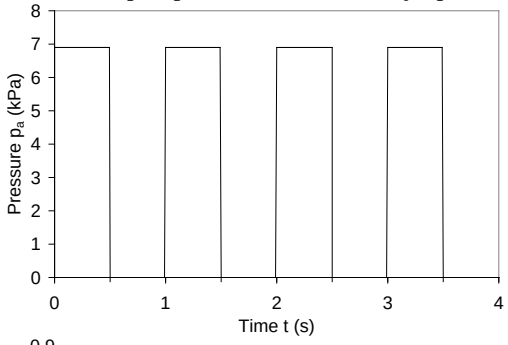

(a)

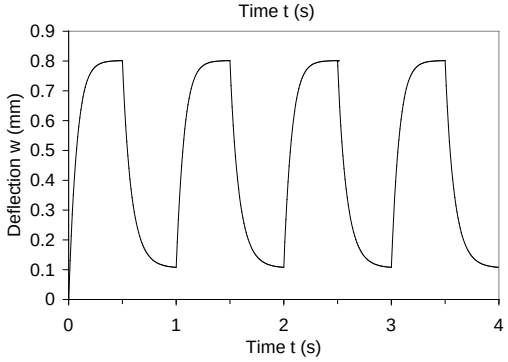

(b)

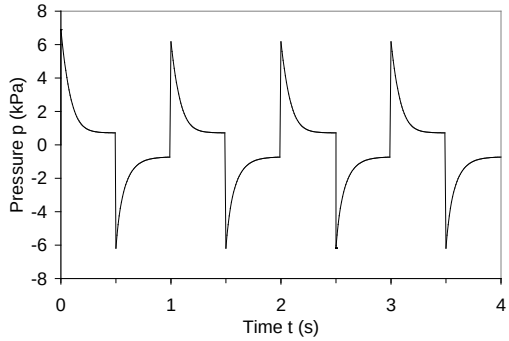

(c)

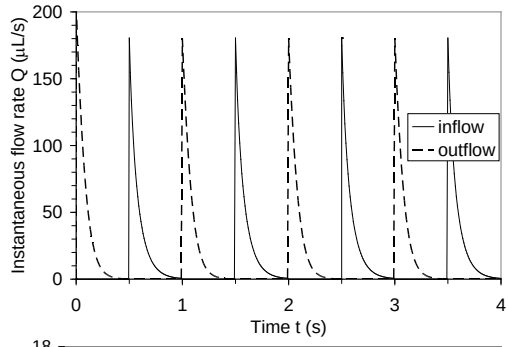

(d)

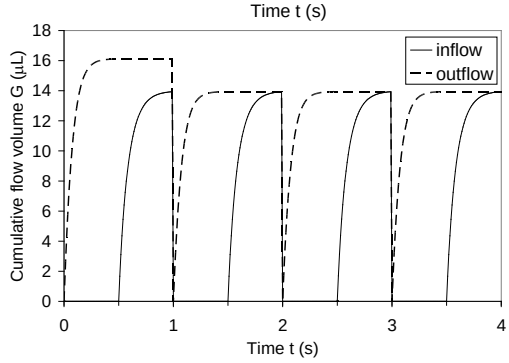

(e)

Figure 5 Simulation results: (a) driving pressure; (b) diaphragm center deflection; (c) pump chamber pressure; (d) instantaneous flow rate; (e) accumulated flow volume.

From the curves of instantaneous flow rate through inlet and outlet in Fig. 5(d), the cumulative fluid volume during a stroke of discharge or suction can be calculated by integration. The results are shown in Fig. 5(e). During the discharge stroke, the cumulative fluid volume through outlet increases from zero to a total volume at the end of this stroke while the cumulative fluid volume through inlet remains zero since there is no flow through inlet during a discharge stroke. During the subsequent suction stroke, the flow through outlet stops already and the corresponding total volume flow through outlet remains the same, while the cumulative fluid volume through inlet increases from zero to a total inlet volume at the end of the stroke. It can be observed in Fig. 5(e) that at the end of the first pump cycle, the cumulative volume through outlet is greater than that through inlet, due to the transient response of the pump. For a stationary operation of a pump, both the final values of the cumulative fluid volumes through inlet and outlet at the end of a cycle should be the same. This value is the fluid volume pumped per cycle.

Figure 6 presents the flow volume pumped per cycle as a function of frequency. As frequency increases, liquid volume

pumped per cycle decreases along a curve resembling a hyperbola. The curve shows that the volume pumped per cycle is inversely proportional to the frequency. The simulation result is compared with experimental data from Meng et al. [21]. It can be observed that the two sets of data agree quite well, especially at low frequency (f = 1–3 Hz).

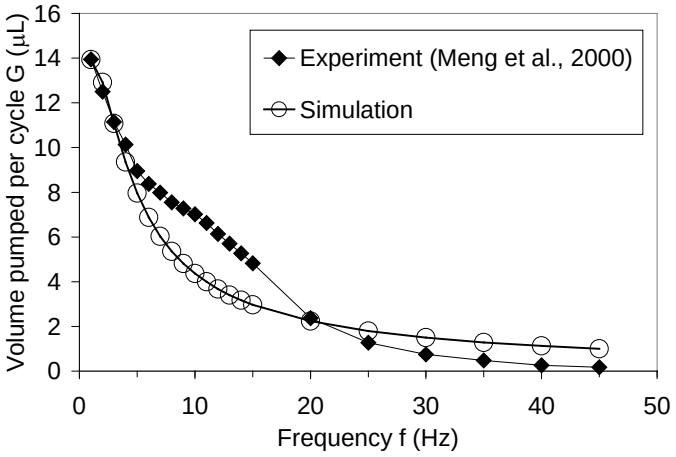

Figure 6 Volume pumped per cycle as function of driving frequency.

Figure 7 shows the flow rate of the micropump as a function of frequency at low frequency up to 4 Hz. Simulated flow rate can be obtained from Eq. (18). As frequency increases, flow rate also increases. It can be observed that flow rate from simulation matches the experimental data almost exactly for frequency of 1, 2 and 3 Hz but begins to depart from each other at 4 Hz. This is well expected since the model was built based on the assumption that the dynamic effects are negligible, which is only valid at low frequency.

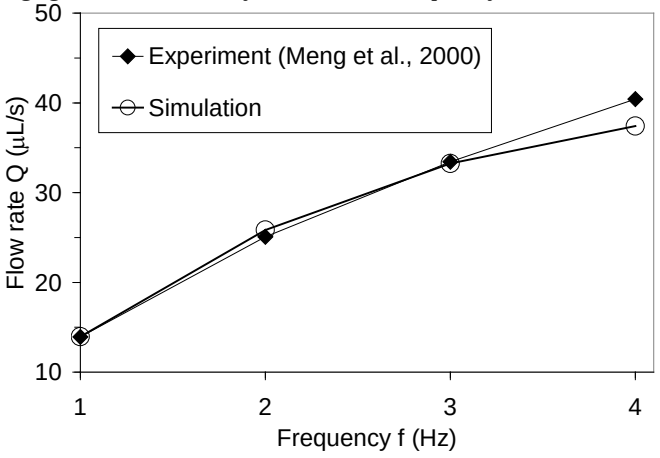

Figure 7 Flow rate as function of driving frequency.

The pumping effect of a diaphragm micropump is produced by the reciprocating motion of the diaphragm that changes the volume of the pump chamber. This volume change in turn creates a pressure that overcomes the critical pressure of the check valve and the backpressure. Flow rate produced by a micropump is therefore dependent on backpressure. Figure 8 shows a comparison between data from simulation and experiment on the relationship of flow rate and backpressure. It can be observed that both curves approximate linear relationships with flow rate decreases as backpressure increases. However, the simulation curve is less steep than the experimental one. A cut-off pressure is defined as one that produces a zero flow rate. The cut-off backpressure from experimental data is about 3.22 kPa while it is 5.47 kPa as predicted from simulation. This can be explained as the results of the fact that the model does not take into account the leak in backward direction through the check valves. It can be verified that the simulated cut-off backpressure can be expressed as $p_{2c} = p_a - p_{v1} - p_{v2} = 6900 - 715 - 715 = 5470$ Pa.

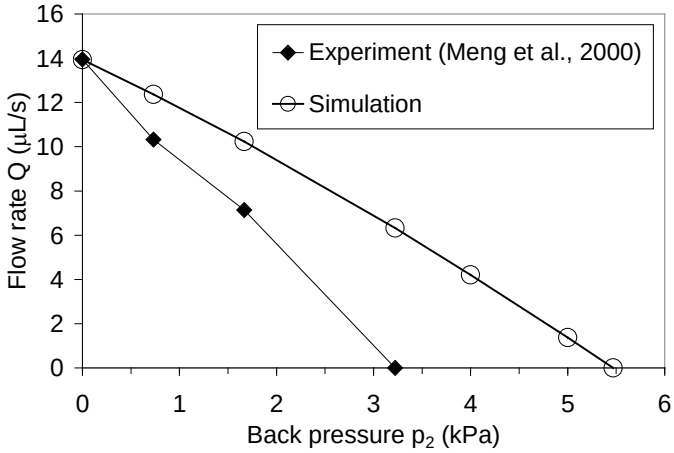

Figure 8 Flow rate as function of back pressure (f = 1 Hz).

The relationship between the cut-off backpressure, the actuating pressure, and the check-valve critical pressure can be expressed as

$$p_{2c} = p_a - p_{v1} - p_{v2} \tag{20}$$

As discussed previously, the critical pressure p_v of the check valves is a parameter that can significantly affect the flow rate Q of the micropump. Figure 9 shows the simulation results of Q as a function of p_v for $p_2 = 0$ and f = 1, 2, and 3 Hz. As p_v increases, Q decreases linearly to zero at the same value of p_v = 3.45 kPa for any frequency considered. The lower limit of p_v is obviously zero, an ideal condition for a check valve that may never be reached. The corresponding flow rate at $p_v = 0$ gives the maximum value of Q that a micropump can produce. The upper limit of p_v where the flow rate becomes zero can also be found from Eq. (20) and the cut-off condition where $p_{2c} = 0$, which leads to $p_v = p_{vc} = p_a/2 = 3.45$ kPa, the same cut-off value as determined by directly running the simulations.

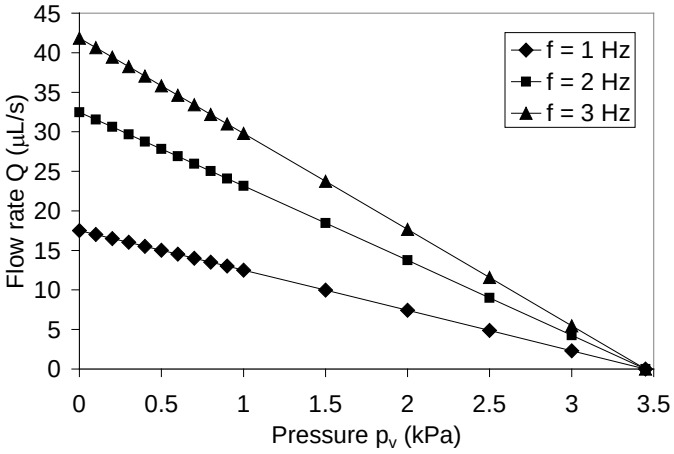

Figure 9 Effect of check valve critical pressure on flow rate.

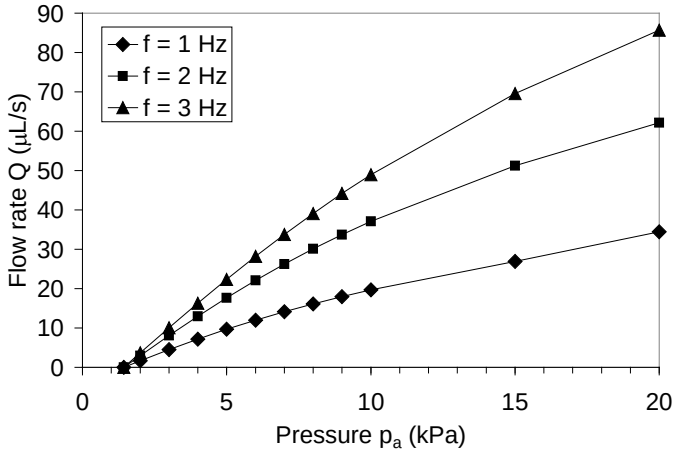

Figure 10 Effect of actuating pressure on flow rate.

Figure 10 presents the simulation results on the dependency of flow rate Q on actuating pressure p_a. It can be observed that the three curves corresponding to f = 1–3 Hz all start at the same point where Q = 0 and $p_a = p_{ac}$ = 1.43 kPa. This cut-off value of p_a, similar to the preceding discussion on p_v and p_{vc}, can also be found from Eq. (20) with p_{2c} = 0 and results in $p_a = p_{ac} = 2p_v$ = 1.43 kPa. As p_a increases as high as the external pneumatic source provides, Q increases monotonically in a slightly nonlinear manner.

Figure 11 shows flow rate Q as a function of the duty cycle ϕ of the pulse train of pneumatic pressure driving the diaphragm. The maximum flow rate is corresponding to a duty cycle of ϕ = 50% for f = 1–3 Hz. As ϕ deviates away from that median in both directions (toward 0% and 100%), Q gradually decreases toward zero. The shape of the curve corresponding to higher frequency more resembles to a concave parabola.

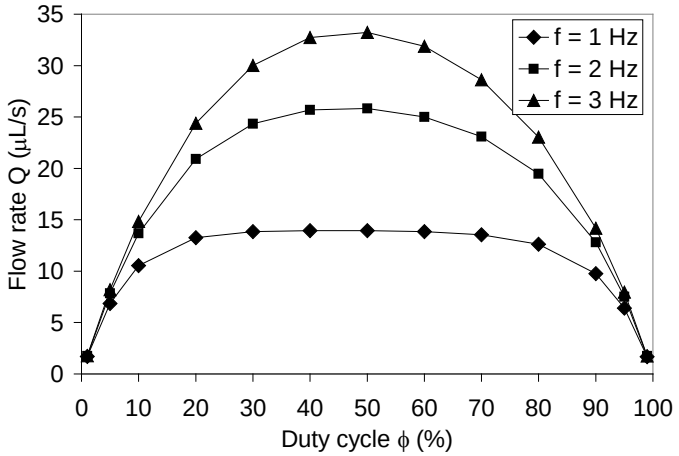

Figure 11 Effect of duty cycle of pulse train of actuating pressure on flow rate.

CONCLUSIONS

A model has been developed for a pneumatically actuated diaphragm micropump with two check valves and one single chamber based on the theories of fluid mechanics and elastic plates and shells. The introduction of the deflection-volume factor ζ of the micropump diaphragm and the bulk modulus K of the working fluid significantly simplifies the modeling. It also results in revealing the relationships between design parameters in the resulting model to be more explicitly visible. Although the mathematical model can be solved using various approaches, the use of the Simulink environment provides a robust yet flexible numerical model that allows the study on the effects of the design parameters to the performance of the micropump interactively.

The model is validated by comparing its simulation results to that of experimental study by Meng et al. [21]. They show good agreements for pump frequency up to 3 Hz. This is well expected since the model is developed with the assumption of quasi-steady operation and without taking into account any dynamic effect. Within 3 Hz frequency, simulated flow rate at zero backpressure fits experimental data well, whereas cut-off backpressure is overestimated by about 2 kPa.

Parametric studies on simulation results allow the predictions on the effects of the operation parameters on micropump performance. For an existing micropump design, where all the geometric and system parameters are fixed, different flow rate can be imposed by setting the magnitude of actuating pressure. The actuating pressure should at least overcome the sum of the critical pressure of both the inlet and outlet check valves. Higher actuating pressure yields higher flow rate. Flow rate can also be adjusted by the duty cycle of the pulse train that produces the reciprocating motion of the diaphragm. At the same magnitude of actuating pressure, a duty cycle of 50% gives the highest flow rate, whereas lower flow

rate is obtained as the duty cycle deviates away from 50% in both directions.

Even though the model is built and validated with the assumption that ζ and K are constant, it can be extended to a more general case where ζ is a function of deflection w, and K is a function of chamber pressure p, provided that these relationships are known from separate studies, either experimental or analytical/numerical, which is quite feasible. The equations of the additional relationships can be integrated conveniently into the present model. Although the present model is developed for a micropump with a pneumatic actuator and passive check valves at inlet/outlet, similar approaches can be employed for the modeling and simulation of diaphragm micropumps with other types of actuator (thermopneumatic, electrostatic, piezoelectric stack, etc.) and passive flow-rectifying valve (nozzle-diffuser, Tesla element, etc.)

ACKNOWLEDGMENTS

This work has been sponsored in whole with federal funds from the National Institute on Alcohol Abuse and Alcoholism, National Institutes of Health under Contract no. N01AA33004.

NOMENCLATURE

A	area of diaphragm, mm²
a	radius of circular diaphragm, mm
B	coefficients (with number subscripts)
C	coefficients (with number subscripts)
D	coefficients (with number subscripts)
E	Young's modulus of diaphragm, Pa
f	pump frequency, Hz
G	cumulative pumped volume in a cycle, mm³ (μL)
h	equivalent height of pump chamber, mm
H	unit step function (Heaviside function)
p	pressure in pump chamber, Pa
p_a	actuating pressure, Pa
p_v	critical pressure of check valve, Pa
Q	flow rate, mm³/s (μL/s)
t	time, s
V	volume of pump chamber, mm³
V_0	nominal volume of pump chamber, mm³
V_d	volume created by deflected diaphragm, mm³
w	deflection at center of diaphragm, mm

Greek letters

Δp	pressure difference, Pa
δ	diaphragm thickness, mm
ζ	diaphragm deflection-volume factor, dimensionless
ν	Poisson's ratio of diaphragm, dimensionless
ρ	density, g/mm³
σ_0	pre-stressed tension of diaphragm, Pa
τ	pump cycle (period), s
Φ	characteristic function of check valve
ϕ	duty cycle , %

Subscripts

1	at inlet
2	at outlet
c	cut-off
in	inflow
out	outflow

REFERENCES

[1] Laser, D. J., and Santiago, J. G., 2004, "A review of micropumps," *J. Micromech. Microeng.*, **14**, pp. R35-R64.

[2] Shoji, S., and Esashi, M., 1994, "Microflow devices and systems," *J. Micromech. Microeng.* **4**, pp. 157-171.

[3] Nguyen, N. –T., Huang, X., and Chuan, T. K., 2002, "MEMS-micropumps: A review," *J. Fluids Eng.*, **124**, pp. 384-392.

[4] Smits, J. G., 1990, "Piezoelectric micropump with three valves working peristaltically," *Sensors Actuators A*, **21**, pp. 203-206.

[5] Knight, M., and House, J., 2004, "Design, fabrication, and test of a peristaltic micropump," *Microsyst. Technol.*, **10**, pp. 426-431

[6] Husband, B., Bu, G., Evans, A. G. R., and Melvin, T., 2004, "Investigation for the operation of an integrated peristaltic micropump," *J. Micromech. Microeng.*, **14**, S64-S69.

[7] Grover, W. H., Skelley, A. M., Liu, C. N., and Lagally, E. T., and Mathies, R. A., 2003, "Monolithic membrane valves and diaphragm pumps for practical large-scale integration into glass microfluidic devices," *Sensors Actuators B*, **89**, pp. 315-323.

[8] Inman, W., Domansky, K., Serdy, J., Owens, B., Trumper, D., and Griffith, L. G., 2007, "Design, modeling and fabrication of a constant flow pneumatic micropump," *J. Micromech. Microeng.*, **17**, pp. 891-899.

[9] Richter, M., Linnemann, R., and Woias, P., 1998, "Robust design of gas and liquid micropumps," *Sensors Actuators A*, **68**, pp. 480-486.

[10] Zengerle, R., and Richter, M., 1994, "Simulation of microfluid systems," *J. Micromech. Microeng.*, **4**, pp. 192-204.

[11] Morris, C. J., and Forster, F. K., 2003, "Low-order modeling of resonance for fixed-valve micropumps based on first principles," *J. Microelectromech. Syst.*, **12**, pp. 325-334.

[12] Bourouina, T., and Grandchamp, J. P., 1996, "Modeling micropumps with electrical equivalent networks," *J. Micromech. Microeng.*, **6**, pp. 398-404.

[13] Olsson, A., Stemme, G., and Stemme, E., 1999, "A numerical design study of the valveless diffuser pump using a lumped-mass model," *J. Micromech. Microeng.*, **9**, pp. 34-44.

[14] Moussa, W. A., and Gonzalez, U. F., 2002, "Simulation of MEMS piezoelectric micropump for biomedical applications," IMECE2002-33602, *Proc. ASME Int. Mechanical Engineering Congress and Exposition (New Orleans, LA).*

[15] Morris, C. J., and Forster, F. K., 2000, “Optimization of a circular piezoelectric bimorph for a micropump driver,” *J. Micromech. Microeng.*, **10**, pp 459-465.

[16] Gerlach, T., 1998, “Microdiffusers as dynamic passive valves for micropump applications,” *Sens. Actuators A*, **69**, pp. 181-191.

[17] Ullman, A., and Fono, I., 2002, “The piezoelectric valve-less pump - improved dynamic model,” *J. Microelectromech. Syst.*, **11**, pp. 655-664.

[18] Pan., L. S., Ng, T. Y., Wu, X. H., and Lee, H. P., 2003, “Analysis of valveless micropumps with inertial effects,” *J. Micromech. Microeng.*, **13**, pp. 390-399.

[19] Gamboa, A. R., Morris, C. J., and Forster, F. K., 2003, “Optimization of the fixed-geometry valve for increased micropump performance,” IMECE2003-55036, *Proc. ASME Fluids Engineering Division*, **259**, pp. 525-534.

[20] Koch, M., Harris, N., Maas, R., Evans, A. G. R., White, N. M., and Brunnschweiler, A., 1997, “A novel micropump design with thick-film piezoelectric actuation,” *Meas. Sci. Technol.*, **8**, pp. 49-57.

[21] Meng, E., Wang, X.-Q., Mak, H., and Tai, Y.-C., 2000, “A check-valved silicone diaphragm pump,” *Proc. MEMS 2000: 13th Annual Int. Conf. on Micro Electro Mechanical Systems* (Miyazaki, Japan), pp. 62–67

[22] Ugural, A. C., 1999, *Stresses in Plates and Shells*, 2nd ed., McGraw-Hill, New York.

[23] Timoshenko, S. P., and Woinowsky-Krieger, S., 1959, *Theory of Plates and Shells*, 2nd ed., McGraw-Hill, New York.

[24] Roark, R. J., and Young, W. C., 1975, *Formulas for Stress and Strain*, 5th ed., McGraw-Hill, New York.

[25] White, F. M., 1991, *Viscous Fluid Flow*, 2nd ed., McGraw-Hill, New York.